Magnetic Resonance Materials in Physics, Biology and Medicine (2019) 32:617–627
https://doi.org/10.1007/s10334-019-00767-x

RESEARCH ARTICLE

Phase-contrast magnetic resonance imaging for analyzing hemodynamic parameters and wall shear stress of pulmonary arteries in patients with pulmonary arterial hypertension

Hung-Hsuan Wang[1] · Wen-Yih Isaac Tseng[2] · Hsi-Yu Yu[3] · Meng-Chu Chang[1] · Hsu-Hsia Peng[1]

Received: 11 December 2018 / Revised: 29 May 2019 / Accepted: 24 June 2019 / Published online: 3 July 2019

Abstract

Objective To investigate flow-related parameters in pulmonary arteries of patients with pulmonary arterial hypertension (PAH).

Materials and methods Eleven PAH patients and twelve control participants were recruited. PAH and controls had similar age and gender distribution. 2D phase-contrast MRI (PC-MRI) was performed in the main, right, and left pulmonary artery (MPA, RPA, and LPA). The flow velocity, wall shear stress (WSS), and oscillatory shear index (OSI) were measured.

Results PAH patients displayed prolonged acceleration time (T_{acce}) and increased ratio of flow change to acceleration volume in pulmonary arteries (both $P<0.001$). The temporally averaged WSS values of MPA, RPA, and LPA in PAH patients were significantly lower than those of control participants ($P<0.001$). The OSI in the pulmonary arteries was higher in PAH patients than control participants ($P<0.05$). The ROC analysis indicated the ratio of maximum flow change to acceleration volume, WSS, and T_{acce} exhibited sufficient sensitivity and specificity to detect patients with PAH. The WSS demonstrated strong correlations with T_{acce} and the ratio value in the two groups ($R^2=0.78$–0.96).

Conclusions We used a clinically feasible 2D PC-MRI sequence with a reasonable scanning time to compute aforementioned indices. The quantitative parameters provided sufficient information to differentiate PAH patients from control participants.

Keywords Pulmonary arterial hypertension · Magnetic resonance imaging · Flow velocity · Wall shear stress

Introduction

Pulmonary arterial hypertension (PAH) is one of the five categories of pulmonary hypertension (PH), and is a progressive condition characterized by progressive obliteration of the pulmonary arterioles, leading to increased pulmonary arterial pressure and eventually to right-ventricular (RV) failure [1]. The underlying mechanism for PAH remains unclear. PAH includes idiopathic PAH (formerly defined as

Presented in part at the 20th and 21st Annual Meetings of the International Society for Magnetic Resonance in Medicine.

Electronic supplementary material The online version of this article (https://doi.org/10.1007/s10334-019-00767-x) contains supplementary material, which is available to authorized users.

✉ Hsu-Hsia Peng
hhpeng@mx.nthu.edu.tw

Hung-Hsuan Wang
b_82733879@hotmail.com

Wen-Yih Isaac Tseng
wytseng@ntu.edu.tw

Hsi-Yu Yu
hsiyuyu@gmail.com

Meng-Chu Chang
v2051917@gmail.com

[1] Department of Biomedical Engineering and Environmental Sciences, National Tsing Hua University, No. 101, Section 2, Kuang-Fu Road, BMES Building, R415, Hsinchu 30013, Taiwan

[2] Institute of Medical Device and Imaging, College of Medicine, National Taiwan University, Taipei, Taiwan

[3] Department of Surgery, National Taiwan University Hospital, Taipei, Taiwan

primary PAH) and PAH associated with the other medical conditions, such as connective tissue diseases and congenital heart diseases. PAH is identified when the mean pulmonary arterial pressure is > 25 mmHg at rest or > 30 mmHg during exercise, and when the pulmonary capillary wedge or left-ventricular end-diastolic pressure is < 15 mmHg and the pulmonary vascular resistance (PVR) is > 3 Wood units [1]. Humber et al. reported a novel risk-prediction equation, combining information on patient sex, 6-minute walking distance, and cardiac output, for estimating the survival of PAH patients [2]. Over the past years, several novel treatment options for PAH have been developed. However, despite the improved survival rate of PAH patients, PAH remains a progressive fatal disease [3]. In PAH, increased PVR leads to RV overload, hypertrophy, and dilatation, and eventually to RV failure and death [4].

The previous studies have used noninvasive phase-contrast magnetic resonance imaging (PC-MRI) to estimate several hemodynamic parameters for diagnosing chronic PH patients. Ley et al. have reported lower pulmonary peak velocity, lower blood flow, shorter time-to-peak velocity, and higher pulmonary velocity rise gradient in the main pulmonary artery (MPA) of PAH patients [5]. A previous study measured stroke volume and cardiac output in the MPA by right-heart catheterization (RHC) and PC-MRI, and has shown a strong correlation between these two schemes [6]. In addition, patients with high PVR have been proven to present inhomogeneous velocity profiles, high retrograde flow, and low distensibility in MPA [6, 7]. Besides, the patients were also associated with shorter acceleration time (T_{acce}) of flow rate in the MPA, lower acceleration volume (V_{acce}), and an increased ratio of maximum upslopes of flow rate to V_{acce} [(maximum dQ/dt)/V_{acce}] during ejection [6]. Nevertheless, aforementioned indices in the right pulmonary artery (RPA) and left pulmonary artery (LPA) have not been discussed thoroughly. The altered flow characteristics of RPA and LPA in PAH patients are still not clear.

In animal experiments, Wang et al. used the Windkessel volume (V_{wk}), which accounts for the shape of the arterial pressure waveform, to describe the reservoir in the aorta by calculating V_{wk} as an integration of the measured inflow (V_{in}) and outflow (V_{out}) during a cardiac cycle [8]. Nonetheless, a step toward elucidating the role of V_{wk} in the system of pulmonary arteries is still deficient.

Because vessels are exposed to various hemodynamics forces, including viscous forces, periodic stretch, and hydrostatic pressure induced by the pulsatile blood flow, several studies have investigated the forces or pressure exerted by the blood flow on the vessel wall to evaluate the specific vascular characteristics of patients. The index of wall shear stress (WSS), which describes the frictional force of the flowing blood on the arterial wall, has attracted increasing attention. Zarins et al. examined postmortem specimens to quantitatively correlate plaque localization with flow velocity profiles and WSS in patients with carotid bifurcation atherosclerosis [9]. The authors concluded that atherosclerosis develops preferentially at branches and curvatures of the arterial tree, which are associated with relatively low WSS, flow separation, and departure from axially aligned, unidirectional flow. Chien et al. indicated that the endothelial cells of vessels bear the majority of the WSS and play a vital role in the remodeling of the vascular wall [10, 11]. Cheng et al. evaluated atherosclerotic lesion size and vulnerability in mouse carotid arteries, observing that reduced shear stress induced larger lesions with a vulnerable plaque phenotype [12]. In addition, Barker et al. calculated the shear range index [13], which is derived from the WSS, to evaluate WSS symmetry along the lumen circumference, observing significant differences in the bicuspid aortic valve between patient and control groups [14]. Stalder et al. used PC-MRI and calculated the oscillatory shear index (OSI) to interpret the temporal oscillation of WSS during the cardiac cycle in healthy volunteers [15].

To date, several schemes have been demonstrated to be able to estimate WSS. Tang et al. developed a combined MRI and computational fluid dynamics (CFD) approach to construct subject-specific pulmonary artery models and to quantify WSS in the MPA of PAH patients [16]. The previous studies reported lower systolic in-plane (i.e., circumferential) WSS values, computed from three-directional velocity-encoding 4D flow data sets, of proximal pulmonary arteries in PAH group [17, 18]. Images acquired with 4D flow MRI may comprise on longer total scanning time and lower spatial resolution for analyzing hemodynamic parameters and WSS.

In this study, we measured blood flow hemodynamic parameters, axial WSS, and WSS-derived OSI in the MPA, RPA, and LPA in PAH patients and control participants using noninvasive time-resolved two-dimensional (2D) PC-MRI. We also investigated the regional distribution of WSS along the circumference of vessel wall. The purpose of this study was to understand the altered flow characteristics of large pulmonary arteries in PAH patients.

Materials and methods

Study cohort

The study population consisted of 11 PAH patients (age 43.0 ± 17.9 years; male/female = 5/6) and 12 control participants without a history of pulmonary disease or pulmonary valve insufficiency (age 38.4 ± 8.9 years; male/female = 5/7). PAH and controls had similar age and gender distribution. Informed consent was obtained from all participants.

MRI acquisition

2D PC-MRI was performed on a 1.5 T clinical scanner (Magnetom Sonata, Siemens, Erlangen, Germany) with a body array coil and prospective ECG triggering. A 2D gradient echo phase-contrast sequence (TR/TE = 11/4.8 ms, flip angle = 15°, temporal resolution = 22 ms, matrix size = 256 × 192, spatial resolution = 1.1 × 1.1 mm^2, and slice thickness = 5 mm) with a 150 cm/s through-plane velocity-encoding gradient was acquired, sampling approximately 90% of the cardiac cycle with free-breathing scheme. Magnitude and phase images of the MPA (about 2 cm proximal to bifurcation), RPA (1–1.5 cm distal to bifurcation), and LPA (1–1.5 cm distal to bifurcation) were obtained. All images were acquired in imaging planes perpendicular to the long axes of the vessels.

Data processing and statistical analysis

Regions of interest (ROIs) were determined manually on magnitude images using a custom-built analysis program written in Matlab (The Mathworks, Natick, USA) [15], and were applied to phase images for calculating the flow velocity (Figure S1). Several parameters including the peak flow rate, the mean flow rate during the cardiac cycle, and the net flow volume were calculated. Figure 1a shows the acceleration time (T_{acce}) of flow rate and the acceleration flow volume (V_{acce}) in a 32-year-old female PAH patient. The T_{acce} was defined as the time from the ECG R-wave to the peak flow rate [6], i.e., the time-to-peak of the flow rate. The integrated flow rate during T_{acce} was defined as V_{acce} [6], as illustrated by the hatched area in Fig. 1a. The max.dQ/dt was the maximum change in the flow rate during ejection, defined by the maximum upslope of the flow rate during systolic phases [6]. We defined a ratio of the two aforementioned parameters to obtain a physical parameter of force exerted by the heart during ejection phases:

$$\text{Ratio} = (\text{max}.dQ/dt)/V_{acce}. \tag{1}$$

To determine the instantaneous change in the windkessel volume (V_{wk}) of the pulmonary system, the integral of the differences between inflow and outflow was calculated, as indicated by the hatched area in Fig. 1b [8].

Several other flow-derived indices were quantified to investigate the hemodynamic differences between the PAH patients and the control participants. The regurgitation fraction was defined as the ratio of the retrograde to antegrade flow volumes [19]. Pulmonary vascular strain was evaluated from magnitude images using the following equation [19]:

$$\text{Vascular strain} = \frac{A_{max} - A_{min}}{A_{min}} \times 100\%, \tag{2}$$

where A_{max} and A_{min} are maximum cross-sectional area and minimum cross-sectional area of the vessel during a cardiac cycle, respectively.

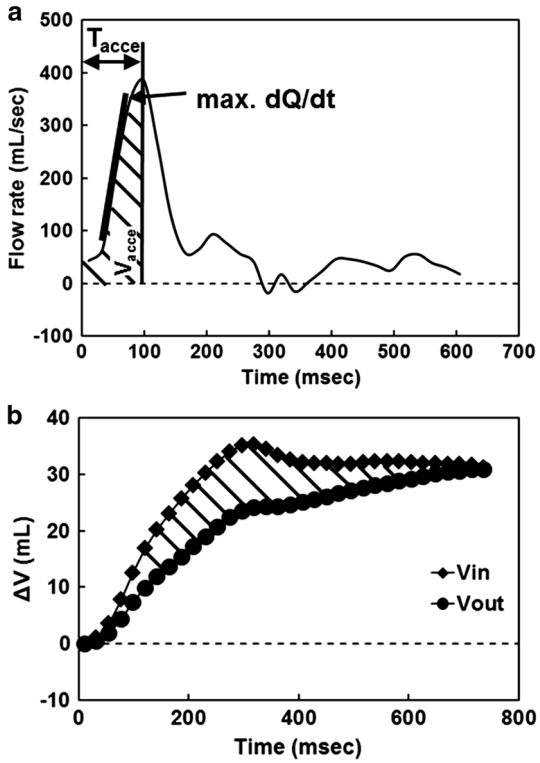

Fig. 1 **a** Several indices derived from the flow profiles are displayed. The T_{acce} was defined as the time duration from the onset of flow to the peak flow rate. The V_{acce} (hatched area) was evaluated by integrating the profile of the flow rate during the T_{acce}. The max.dQ/dt during the systolic phase was evaluated as the maximum slope of the flow rate curve (thick solid line). **b** Integrals of pulmonary aerial inflow (V_{in}) and outflow (V_{out}) in a 45-year-old female PAH patient. The integral of the differences between the inflow (MPA) and outflow (RPA and LPA) represents the instantaneous change in the V_{wk} (hatched area) during a cardiac cycle

Because PAH patients can exhibit abnormal shear stress in the pulmonary arteries, axial WSS estimations (or $\vec{\tau}$), i.e., the WSS along the main flow direction, were performed. As described in the previous study [15], if a 1D problem is considered, the estimations of $\vec{\tau}$ can be simplified to the following:

$$\vec{\tau} = \eta \frac{\partial v}{\partial h}, \tag{3}$$

where η denotes the dynamic viscosity and was assumed as 4.5 cP [15], v denotes the blood flow velocity, and h denotes the height of boundary. As described by Stalder et al., this calculation combines Green's theorem and B-spline interpolation to provide an optimal quantification of several blood flow and vessel wall parameters [15].

To determine the temporal oscillation in WSS during a cardiac cycle, the OSI was calculated as follows:

$$\text{OSI} = \frac{1}{2}\left(1 - \frac{\left|\int_0^T \vec{\tau} \cdot dt\right|}{\int_0^T \left|\vec{\tau}\right| \cdot dt}\right), \tag{4}$$

where T is the duration of the cardiac cycle and $\vec{\tau}$ is the instantaneous WSS vector as given by Eq. (3) [15].

The unpaired Student's t test (two-tailed) was used to evaluate the significance of differences between the PAH patients and the control participants. We also analyzed the receiver-operating characteristic (ROC) curves of several quantified indices by the software of SPSS 12 (SPSS, Chicago, IL). The area under the ROC curve (AUC), cut-off value, specificity, sensitivity, and accuracy were determined to perform the diagnostic performance of each index. The Pearson's correlation analysis was performed to correlate WSS with peak flow rate, T_{acce}, and the ratio. A P value < 0.05 was considered statistically significant.

Results

Blood flow hemodynamic indices

Figure 2 shows the time courses of the pulmonary flow rates in the MPA, RPA, and LPA throughout the cardiac cycles of a control participant (age 32 years, female) and a PAH patient (age 32 years, female). In comparison with the control participants, the PAH patients displayed markedly increased flow rates in the MPA, RPA, and LPA, which indicated that the flow patterns differed between the two groups. However, the mean flow volumes and peak flow rate of PAH patients and control participants showed non-significant difference (Table 1). The measured T_{acce} values of the control participants and the PAH patients were 132.1 ± 14.0 ms and 93.8 ± 22.6 ms in the MPA, 148.4 ± 20.4 ms, and 99.2 ± 19.8 ms in the RPA, and 136.7 ± 28.6 ms and 96.0 ± 17.6 ms in the LPA (all $P < 0.001$), respectively (Fig. 3a). As shown in Fig. 3b, the V_{acce} differed significantly between the two groups only in the LPA (control participant 6.4 ± 1.5 cm^3, PAH patient 4.0 ± 3.4 cm^3; $P < 0.05$). We observed markedly higher systolic max.dQ/dt values (Fig. 3c) in the MPA and RPA in the PAH patients (6.5 ± 3.4 L/s^2 and 2.9 ± 1.8 L/s^2) than in the control participants (4.0 ± 1.2 L/s^2 and 1.7 ± 0.6 L/s^2), as reflected by the steeper upslope of the flow rate curves in the PAH patient (Fig. 2b). The defined ratio of normalized maximum systolic increase in the flow rate is a physical parameter that demonstrates the force exerted by the heart during ejection phases. As shown in Fig. 3d, the PAH patients exhibited significantly higher values for this parameter in the MPA, RPA, and LPA than the control participants [MPA: 373.0 ± 101.0 s^{-2} vs. 189.5 ± 65.7 s^{-2}, RPA: 434.8 ± 139.4 s^{-2} vs. 195.8 ± 70.3 s^{-2}, and LPA: 553.5 ± 224.5 s^{-2} vs. 214.9 ± 98.5 s^{-2} (all $P < 0.001$)].

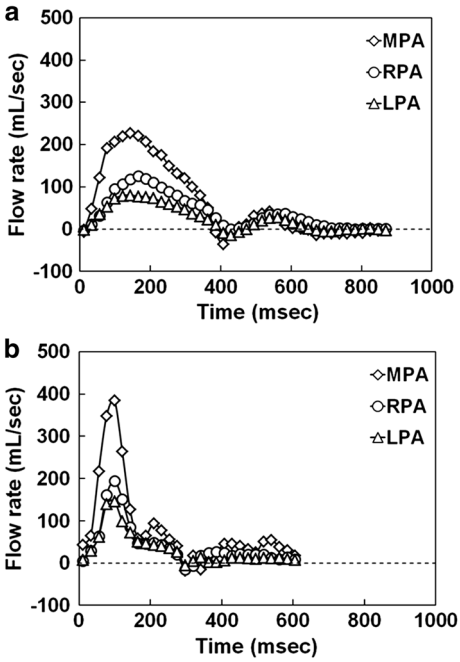

Fig. 2 The time courses of the pulmonary flow rates in the pulmonary arteries throughout the cardiac cycle in **a** a 32-year-old female control participant and **b** a 32-year-old female PAH patient

WSS, OSI, and other indices

Figure 4 shows the time courses of WSS in the MPA, RPA, and LPA in the control participants and PAH patients. The PAH group exhibited lower WSS values than the control group. The box plots in Fig. 5a, b show the hemodynamic indices of the WSS and WSS-derived OSI in the control participants and PAH patients. The temporally averaged WSS (Fig. 5a) in the MPA of the PAH patients was 0.21 ± 0.06 N/m^2, which was considerably lower than that in the control participants (0.28 ± 0.04 N/m^2, $P < 0.001$). We observed the same trend in the RPA and the LPA. The OSI in the RPA ($17.7 \pm 8.5\%$ vs. $10.2 \pm 4.0\%$, $P < 0.01$) and LPA ($21.9 \pm 9.3\%$ vs. $15.3 \pm 4.3\%$, $P < 0.05$) displayed significantly higher values in PAH patients compared to control participants.

The mean values of vascular strain in the control participants (MPA: $28.4 \pm 13.3\%$; LPA: $34.2 \pm 16.4\%$) were significantly higher than those in the PAH patients (MPA: $13.1 \pm 4.7\%$; LPA: $20.5 \pm 9.0\%$), suggesting that the vessel walls of the control participants were less stiff than those of the PAH patients (Fig. 5c). The PAH patients exhibited a regurgitation fraction of $6.4 \pm 6.0\%$ in the MPA, which was higher than that of the control participants ($1.5 \pm 1.5\%$, $P < 0.05$), indicating increased retrograde flow in the patients with PAH compared with the control participants (Fig. 5d). The V_{wk} of the PAH patients and control participants showed non-significant differences (Fig. 5e). Table 1 summarizes

Table 1 Hemodynamic parameters in the MPA, RPA, and LPA in the control and PAH groups

Parameter	MPA	RPA	LPA
Area (mm^2)			
Control	517.0 ± 62.0	216.6 ± 49.5	185.6 ± 45.2
PAH	893.5 ± 264.4***	399.4 ± 173.3**	333.6 ± 131.2**
Peak flow rate (mL/s)			
Control	268.6 ± 60.1	123.4 ± 25.1	90.5 ± 29.4
PAH	364.3 ± 176.0	158.5 ± 93.9	91.2 ± 50.6
Flow volume (mL)			
Control	63.1 ± 12.2	30.0 ± 5.5	21.7 ± 6.7
PAH	50.0 ± 22.4	29.1 ± 15.0	13.4 ± 10.3*
T_{acce} (ms)			
Control	132.1 ± 14.0	148.4 ± 20.4	136.7 ± 28.6
PAH	93.8 ± 22.6***	99.2 ± 19.8***	96.0 ± 17.6***
V_{acce} (cm^3)			
Control	22.0 ± 7.2	9.2 ± 2.3	6.4 ± 1.5
PAH	18.7 ± 10.0	7.2 ± 2.3	4.0 ± 3.4*
Max. dQ/dt (L/s^2)			
Control	4.0 ± 1.2	1.7 ± 0.6	1.3 ± 0.6
PAH	6.5 ± 3.4*	2.9 ± 1.8*	1.7 ± 0.9
Ratio (s^{-2})			
Control	189.5 ± 65.7	195.8 ± 70.3	214.9 ± 98.5
PAH	373.0 ± 101.0***	434.8 ± 139.4***	553.5 ± 224.5***
Wall shear stress (N/m^2)			
Control	0.28 ± 0.04	0.33 ± 0.11	0.32 ± 0.06
PAH	0.21 ± 0.06***	0.19 ± 0.06***	0.18 ± 0.06***
Oscillatory shear index (%)			
Control	16.6 ± 6.4	10.2 ± 4.0	15.3 ± 4.3
PAH	22.2 ± 7.0	17.7 ± 8.5*	21.9 ± 9.3*
Vascular strain (%)			
Control	28.4 ± 13.3	46.8 ± 24.7	34.2 ± 16.4
PAH	13.1 ± 4.7**	31.6 ± 11.0	20.5 ± 9.0*
Regurgitation fraction (%)			
Control	1.5 ± 1.5	0.8 ± 1.1	2.9 ± 4.1
PAH	6.4 ± 6.0*	2.5 ± 4.9	7.8 ± 10.1
	Control	PAH	
V_{wk} (cm^3)	10.5 ± 4.8	9.8 ± 6.8	

Values are presented as mean ± standard deviation

*$P < 0.05$, **$P < 0.01$, ***$P < 0.001$

the hemodynamic parameters of the MPA, RPA, and LPA in the two groups.

Segmental WSS

Figure 6 illustrates the regional distribution of WSS along the circumference of the vessel wall. The PAH patients generally exhibited lower segmental WSS in the MPA, RPA, and LPA than the control participants. In the RPA, the WSS in the segments in head–posterior–foot orientation (Fig. 6, middle column) were markedly lower in the PAH patients than in the control participants ($P < 0.001$). In the LPA, the WSS in all segments were significantly lower in the PAH patients than in the control participants. The segmental WSS values in the RPA and LPA of the PAH patients were approximately 50% of those of the control participants (Fig. 6, middle and right columns).

Both groups exhibited inhomogeneous WSS distribution, particular in control group, which may be attributable to uneven flow velocity profiles. Lower segmental variations of WSS in PAH group indicated reduced asymmetry of WSS along the circumference of the vessel walls.

ROC curve analysis and correlation analysis

Figure 7 presents the ROC curves in MPA, RPA, and LPA for the quantified indices showing significant difference between PAH and control groups. Table 2 summarizes the ROC curve-related parameters. In MPA, the defined ratio, WSS, and T_{acce} displayed high AUC (all AUC > 0.85) and sufficient sensitivity (70–90.9%) and specificity (91.7–100%), all with $P < 0.005$. Similar trends can be observed in RPA and LPA.

As shown in Fig. 8, either in PAH patients or control participants, WSS demonstrated strong correlations with T_{acce} ($R^2 = 0.87$–0.96) and the ratio ($R^2 = 0.78$–0.94).

Discussion

In this study, we performed 2D PC-MRI to quantify several flow-derived hemodynamic parameters, WSS, and WSS-derived OSI parameters in MPA, RPA, and LPA, and used them to differentiate the PAH patients from the control participants. The integrated information of abovementioned indices can help to understand the altered flow characteristics of large pulmonary arteries in PAH patients.

The reduced T_{acce} in the MPA, RPA, and LPA of PAH patients demonstrated the effects of high PVR on the pumping function of the right heart. The V_{acce} in the MPA and RPA showed no significant difference between PAH patients and control participants. It may be attributed to a compensatory effect in which the heart provides sufficient V_{acce} during systolic phases, even in the presence of high pressure and resistance in the pulmonary system in PAH patients. Increased maximum dQ/dt values in the PAH group suggested that the flow rate reached a maximum within a shorter period in the PAH patients than in the control participants. The PAH patients also exhibited higher values for the ratio than the control participants, indicating that the right heart might exert a larger force in PAH than in normal condition to resist high-pressure gradient and resistance in the pulmonary system. The high accuracy in the ROC analysis in the defined ratio and T_{acce} further illustrated their diagnostic

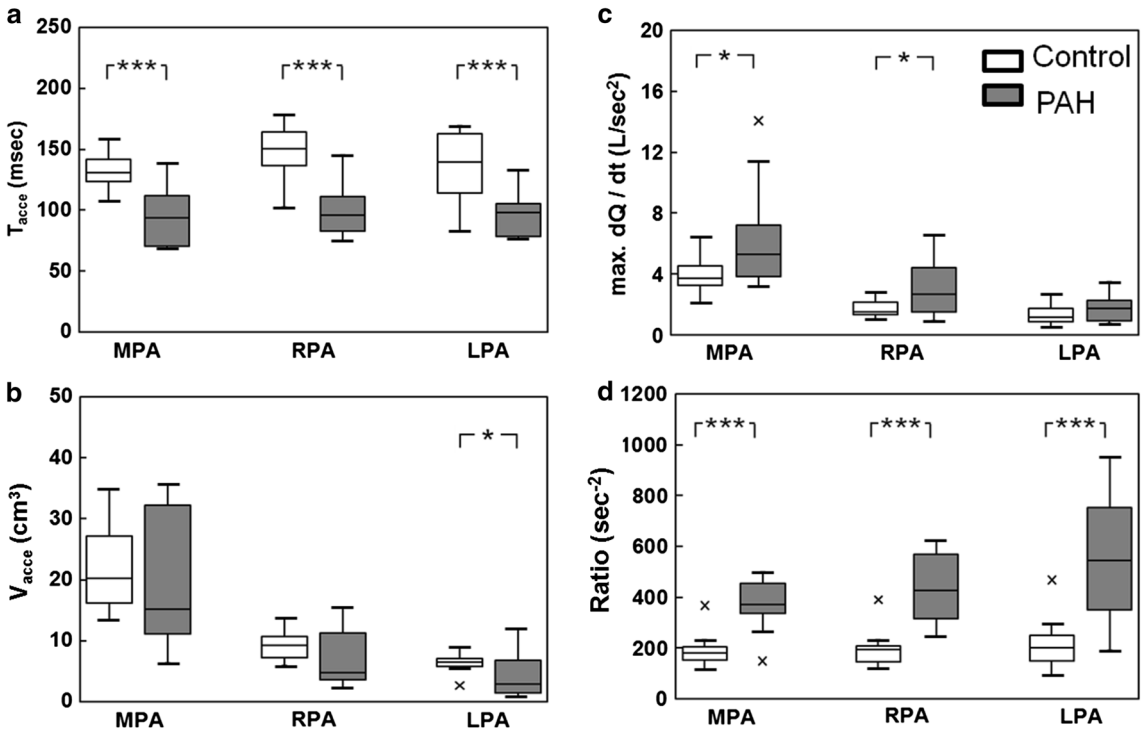

Fig. 3 The box plots show the **a** T_{acce}, **b** V_{acce}, **c** max.dQ/dt, and **d** the defined ratio in the MPA, RPA, and LPA of the control participants (white box) and the PAH patients (grey box). $^{*}P<0.05$, $^{***}P<0.001$

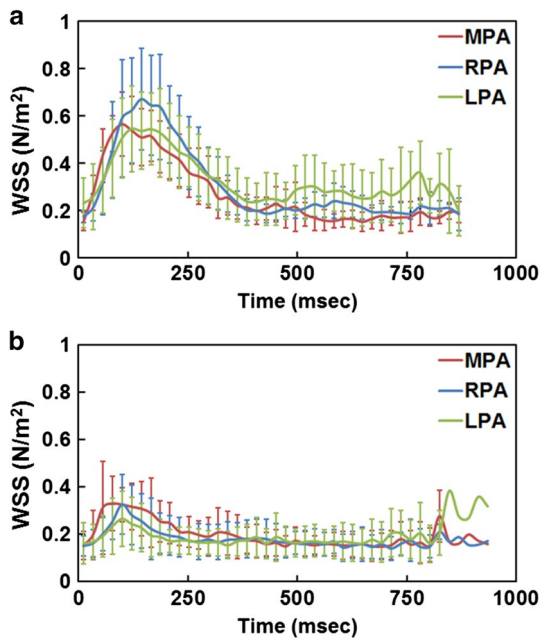

Fig. 4 The time courses of the WSS in the MPA, RPA, and LPA of **a** the control participants and **b** the PAH patients. The error bars indicate the standard deviation of WSS values in the control or PAH groups

powers to demonstrate the abnormality in the large pulmonary arteries of PAH patients.

The PAH patients exhibited lower pulmonary vascular strain in the MPA and LPA compared with the control participants, suggesting that PAH is associated with increased stiffness in the pulmonary arteries, which is consistent with the results of previous histopathological research [20].

Wang et al. indicated that V_{wk} can be used to estimate aortic arterial compliance [8]. However, in our preliminary results, the V_{wk} values of the control and PAH groups were indistinguishable, which may have resulted from variations in the treatment phases and progression of the PAH patients. Therefore, the V_{wk} index may not provide a robust parameter for assessing PAH in our present results. In future investigation of the V_{wk} index, recruiting a larger population of PAH patients and separating the patients subject to various treatment phases and progression into subgroups are necessary.

The previous studies have demonstrated that shear stress induced by laminar blood flow plays an essential role in normal vascular functioning, which includes the regulation of the vascular caliber as well as the inhibition of the proliferation, thrombosis, and inflammation of the vessel wall [9, 10, 21–23]. Sustained high shear stress can modulate the expression of vascular endothelial cell genes and proteins that protect against atherosclerosis. Butler et al. indicated that the temporal gradient in shear stress is essential for the modulation of signaling and gene expression in

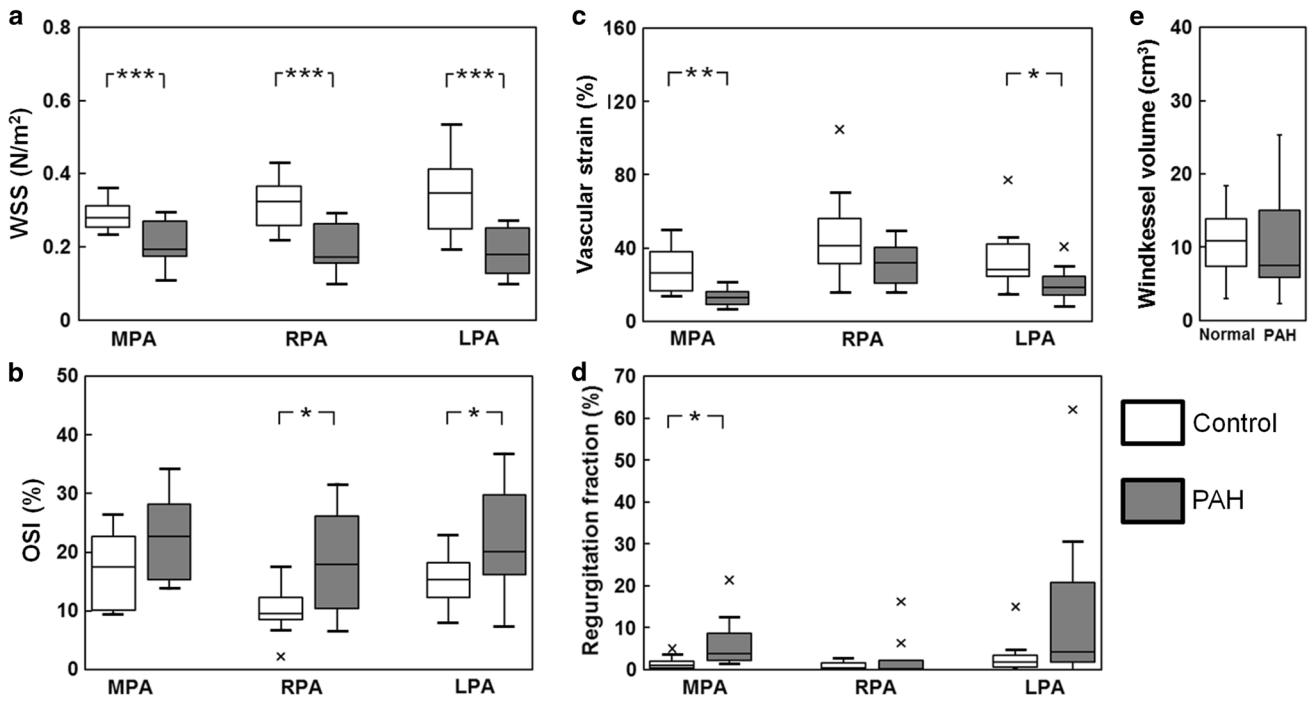

Fig. 5 The box plots show the calculated hemodynamic indices of **a** WSS, **b** OSI, **c** vascular strain, and **d** regurgitation fraction in the control participants (white box) and the PAH patients (grey box). **e** The V_{wk} of the control and PAH group. $^{*}P<0.05$, $^{**}P<0.01$, $^{***}P<0.001$

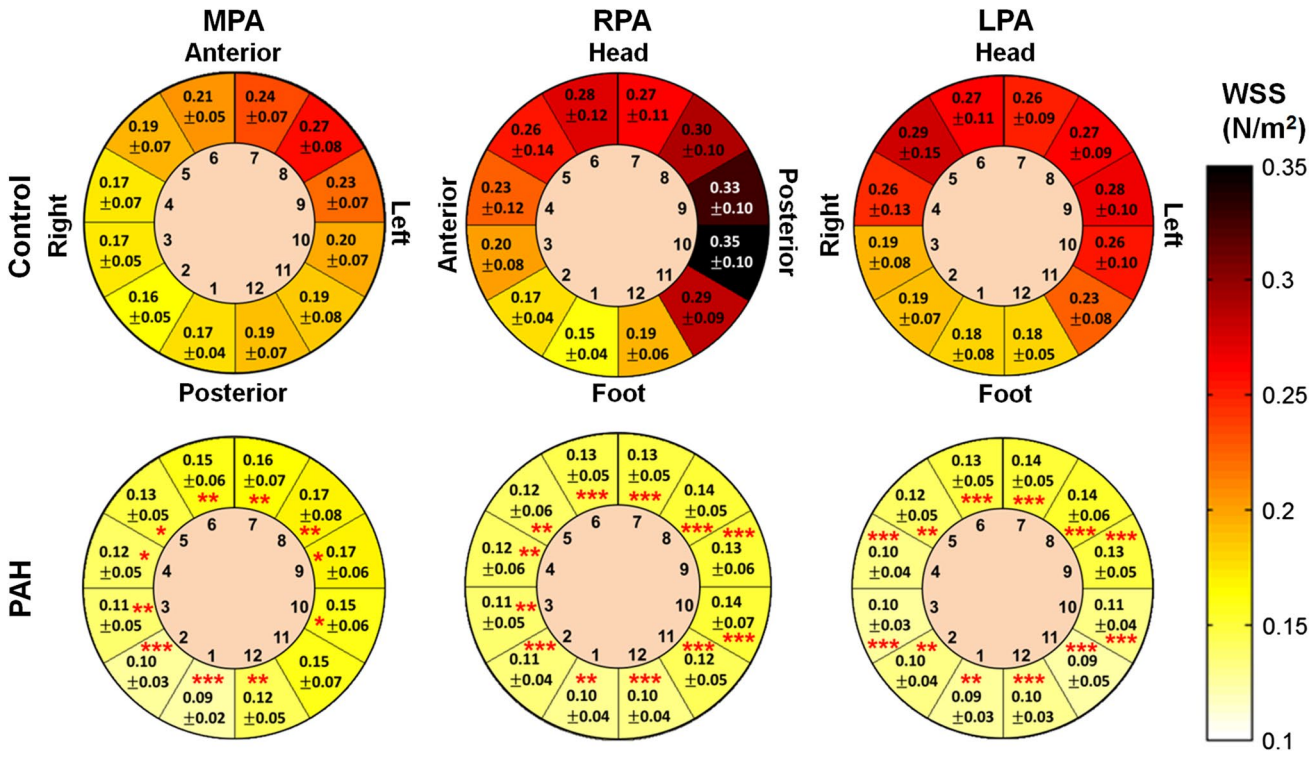

Fig. 6 The regional distributions of the WSS along the circumference of the MPA, RPA, and LPA during a cardiac cycle in control participants and PAH patients

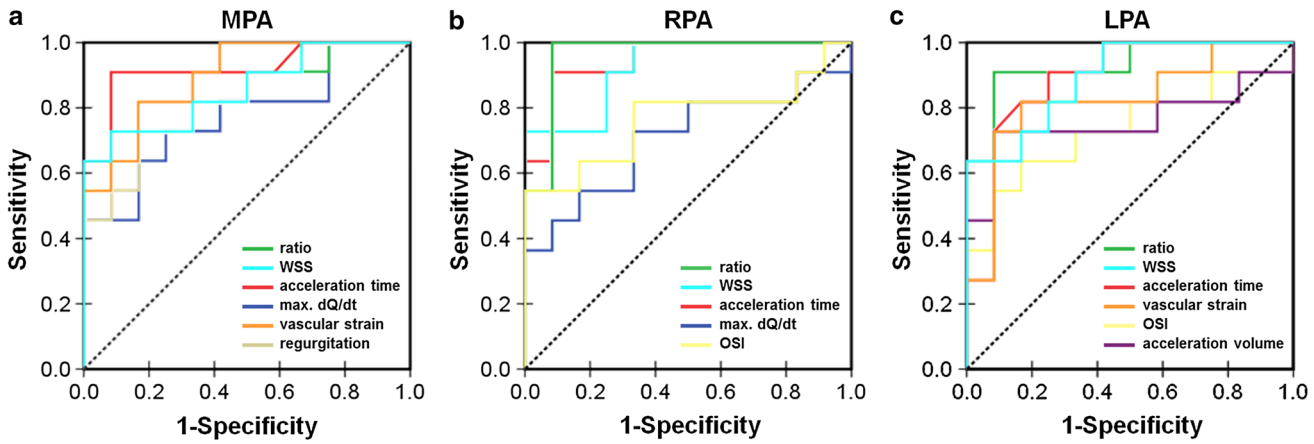

Fig. 7 The ROC curves in MPA, RPA, and LPA for the quantified indices showing significant difference between PAH and control groups

Table 2 The ROC analysis of hemodynamic parameters in MPA, RPA, and LPA

Index	AUC	*P* value	Cut-off value	Specificity (%)	Sensitivity (%)	Accuracy (%)
MPA						
Ratio (s^{-2})	0.902	0.0011	248	91.7	90.9	91.3
WSS (N/m^2)	0.850	0.0056	0.23	100.0	70.0	85.6
Acceleration time (s)	0.921	0.0009	0.11	91.7	90.0	90.8
Max. dQ/dt (L/s^2)	0.773	0.0267	4.41	75.0	72.7	73.9
Vascular strain (%)	0.900	0.0016	16	83.3	80.0	81.7
Regurgitation (%)	0.879	0.0021	2.2	83.3	81.8	82.6
RPA						
Ratio (s^{-2})	0.962	0.0002	238	91.7	100.0	95.6
WSS (N/m^2)	0.917	0.0010	0.20	100.0	70.0	85.6
Acceleration time (s)	0.950	0.0004	0.12	91.7	90.0	90.8
Max. dQ/dt (L/s^2)	0.705	0.0966	1.73	66.7	72.7	69.5
OSI (%)	0.765	0.0312	17.73	100.0	54.5	78.2
LPA						
Ratio (s^{-2})	0.932	0.0005	316	91.7	90.9	91.3
WSS (N/m^2)	0.900	0.0016	0.18	100.0	70.0	85.6
Acceleration time (s)	0.888	0.0022	0.11	75.0	90.0	82.1
Distensibility (%)	0.817	0.0122	24	83.3	80.0	81.7
OSI (%)	0.735	0.0564	19.1	83.3	63.6	73.9
Acceleration volume (mL)	0.742	0.0559	4.3	91.7	70.0	81.3

vascular endothelial cells and their associated vasodilation function [24]. Because disturbed blood flow and associated low shear stress may upregulate the expression of genes and proteins involved in vessel remodeling, we evaluated the differences in WSS in the large pulmonary arteries of PAH patients, attempting to understand the abnormal WSS in MPA, PRA, and LPA in patient group. In the PAH patients, reduced WSS during systolic phases as well as reduced temporally averaged WSS throughout the cardiac cycle may upregulate the expression of genes involved in vasoconstriction in the pulmonary vascular system. Increased OSI, representing increased oscillations in WSS, can further indicate disturbed flow patterns in the MPA, RPA, and LPA of the PAH patients. A heterogeneous flow velocity may result in heterogeneous direction of the WSS, leading to reduced WSS. Accordingly, the disturbance in flow, the reduction in WSS, and the increase of OSI may, consequently, have integrated impact on vasoconstriction in PAH patients. On the other hand, the high correlations showing between WSS and the defined ratio or T_{acce} further described the interaction of abnormal vascular characteristics and altered blood flow.

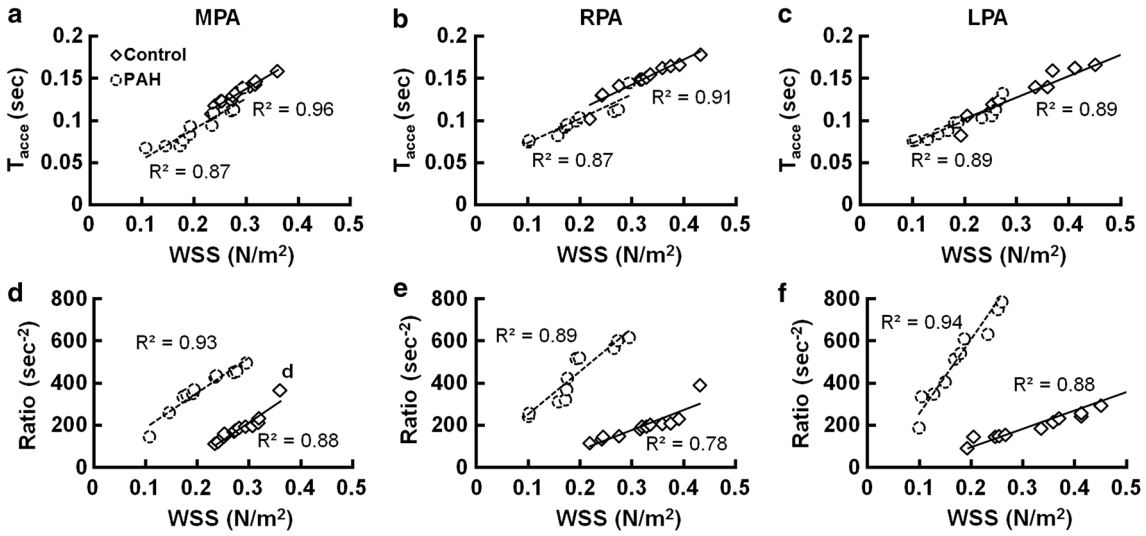

Fig. 8 The correlations between WSS and T_{acce} (**a**–**c**) and the defined ratio of (max. dQ/dt)/V_{acce} (**e**, **f**)

Detailed investigation of the segmental WSS may also provide useful information for assessing PAH. In each segment, the PAH group presented lower WSS compared to the control group, especially at segments 1–2 (posterior-right orientation) in the MPA, segments 6–12 (head–posterior–foot orientation) in the RPA, and segments 6–12 (head–left-foot orientation) in the LPA. The previous studies have indicated that atherosclerotic lesions typically occur in the regions of curvature and bifurcation of the arteries where they are usually with low WSS values [9, 25]. Therefore, in our study, the segments in regions with low WSS might be associated with a high risk of damage to vascular wall. Future investigations of segmental WSS in PAH are warranted to provide sophisticated information for clinical assessment.

There are several limitations in this study. First, to achieve a high temporal resolution and to shorten scanning time, we acquired images using time-resolved 2D PC-MRI and acquired data only on through-plane flow velocity-encoding. Bollache et al. reported that one-directional velocity-encoding technique may present lower flow measurements than that measured by three-directional velocity-encoding scheme [26]. Therefore, acquiring three-directional velocity-encoding flow data can provide additional useful information for PAH assessment, such as circumferential WSS of vessel walls [15] or path lines of pulmonary vascular flow in the case of 4D flow data acquisition [13, 27]. Second, considering the total scanning time, we did not evaluate the routine cardiac function in this study. Obtaining measurements on RV morphology and function to calculate geometry- and function-derived indices [28, 29] may also increase the usefulness of the measured parameters in assessing PAH. Using parallel imaging and navigator-controlled respiration scheme may enable the acquisition of images with higher temporal resolution or spatial resolution, providing subtle details on the temporal and spatial variations between the PAH patients and control participants. Third, the limited numbers of study participants and without correction of momentary situation may not exclude the possible confounding factors of WSS; for example, blood pressure, heart rate, medication, as well as smoking situation. In future studies, the above-mentioned factors and other physiological parameters, such as pulmonary vascular resistance or pulmonary pressure, can be considered altogether to establish a risk-prediction model for PAH patients. Fourth, the lack of catheterization data may limit the understanding of the correlation between computed indices and clinical outcome.

In conclusion, we evaluated several hemodynamic parameters, WSS, and WSS-derived OSI using 2D PC-MRI images in a clinically feasible scanning time and without using complex post-processing procedures. Our results indicated that these indices are of assessing relevance in PAH and enable the differentiation of PAH patients from control participants. The establishment of these indices for PAH may facilitate the long-term follow-up of the treating efficacy and management of PAH patients.

Acknowledgements This study was funded by the National Science Council, Taiwan (NSC 102-2320-B-007-003-MY3; MOST 106-2314-B-007-006-MY3) and Veterans General Hospitals and University System of Taiwan Joint Research Program (VGHUST103-G3-1-1).

Funding This study was funded by the Ministry of Science and Technology, Taiwan (NSC 102-2320-B-007-003-MY3; MOST 106-2314-B-007-006-MY3) and Veterans General Hospitals and University System of Taiwan Joint Research Program (VGHUST103-G3-1-1).

Compliance with ethical standards

Conflict of interest The authors declare that they have no conflict of interest.

Informed consent Informed consent was obtained from all individual participants included in the study.

Ethical approval All procedures performed in studies involving human participants were in accordance with the ethical standards of the institutional and/or national research committee and with the 1964 Helsinki declaration and its later amendments or comparable ethical standards.

References

1. Chin KM, Rubin LJ (2008) Pulmonary arterial hypertension. J Am Coll Cardiol 51(16):1527–1538
2. Humbert M, Sitbon O, Yaici A, Montani D, O'Callaghan DS, Jais X, Parent F, Savale L, Natali D, Gunther S, Chaouat A, Chabot F, Cordier JF, Habib G, Gressin V, Jing ZC, Souza R, Simonneau G (2010) Survival in incident and prevalent cohorts of patients with pulmonary arterial hypertension. Eur Respir J 36(3):549–555
3. Humbert M, Sitbon O, Chaouat A, Bertocchi M, Habib G, Gressin V, Yaici A, Weitzenblum E, Cordier JF, Chabot F, Dromer C, Pison C, Reynaud-Gaubert M, Haloun A, Laurent M, Hachulla E, Cottin V, Degano B, Jais X, Montani D, Souza R, Simonneau G (2010) Survival in patients with idiopathic, familial, and anorexigen-associated pulmonary arterial hypertension in the modern management era. Circulation 122(2):156–163
4. Batt J, Shadly Ahmed S, Correa J, Bain A, Granton J (2013) Skeletal muscle dysfunction in idiopathic pulmonary arterial hypertension. Am J Respir Cell Mol Biol
5. Ley S, Mereles D, Puderbach M, Gruenig E, Schock H, Eichinger M, Ley-Zaporozhan J, Fink C, Kauczor HU (2007) Value of MR phase-contrast flow measurements for functional assessment of pulmonary arterial hypertension. Eur Radiol 17(7):1892–1897
6. Mousseaux ETJ, Jolivet O, Simonneau G, Bittoun J, Gaux JC (1999) Pulmonary arterial resistance: noninvasive measurement with indexes of pulmonary flow estimated at velocity-encoded MR imaging—preliminary experience1. Radiology 212:896–902
7. Kondo C, Caputo GR, Masui T, Foster E, O'Sullivan M, Stulbarg MS, Golden J, Catterjee K, Higgins CB (1992) Pulmonary hypertension: pulmonary flow quantification and flow profile analysis with velocity-encoded cine MR imaging. Radiology 183(3):751–758
8. Wang JJOBA, Shrive NG, Parker KH, Tyberg JV (2003) Time-domain representation of ventricular-arterial coupling as a windkessel and wave system. Am J Physiol Heart Circ Physiol 284(4):H1358–H1368
9. Zarins CK, Giddens DP, Bharadvaj BK, Sottiurai VS, Mabon RF, Glagov S (1983) Carotid bifurcation atherosclerosis. Quantitative correlation of plaque localization with flow velocity profiles and wall shear stress. Circ Res 53(4):502–514.
10. Chien S (2007) Mechanotransduction and endothelial cell homeostasis: the wisdom of the cell. Am J Physiol Heart Circ Physiol 292(3):H1209–1224
11. Chien S, Li S, Shyy YJ (1998) Effects of mechanical forces on signal transduction and gene expression in endothelial cells. Hypertension 31(1 Pt 2):162–169
12. Cheng C, Tempel D, van Haperen R, van der Baan A, Grosveld F, Daemen MJ, Krams R, de Crom R (2006) Atherosclerotic lesion size and vulnerability are determined by patterns of fluid shear stress. Circulation 113(23):2744–2753
13. Francois CJ, Srinivasan S, Schiebler ML, Reeder SB, Niespodzany E, Landgraf BR, Wieben O, Frydrychowicz A (2012) 4D cardiovascular magnetic resonance velocity mapping of alterations of right heart flow patterns and main pulmonary artery hemodynamics in tetralogy of Fallot. J Cardiovasc Magn Reson 14:16
14. Barker AJ, Lanning C, Shandas R (2010) Quantification of hemodynamic wall shear stress in patients with bicuspid aortic valve using phase-contrast MRI. Ann Biomed Eng 38(3):788–800
15. Stalder AF, Russe MF, Frydrychowicz A, Bock J, Hennig J, Markl M (2008) Quantitative 2D and 3D phase contrast MRI: optimized analysis of blood flow and vessel wall parameters. Magn Reson Med 60(5):1218–1231
16. Tang BT, Pickard SS, Chan FP, Tsao PS, Taylor CA, Feinstein JA (2012) Wall shear stress is decreased in the pulmonary arteries of patients with pulmonary arterial hypertension: an image-based, computational fluid dynamics study. Pulm Circ 2(4):470–476
17. Barker AJ, Roldan-Alzate A, Entezari P, Shah SJ, Chesler NC, Wieben O, Markl M, Francois CJ (2015) Four-dimensional flow assessment of pulmonary artery flow and wall shear stress in adult pulmonary arterial hypertension: results from two institutions. Magn Reson Med 73(5):1904–1913
18. Schafer M, Kheyfets VO, Schroeder JD, Dunning J, Shandas R, Buckner JK, Browning J, Hertzberg J, Hunter KS, Fenster BE (2016) Main pulmonary arterial wall shear stress correlates with invasive hemodynamics and stiffness in pulmonary hypertension. Pulm Circ 6(1):37–45
19. Tardivon AA, Mousseaux E, Brenot F, Bittoun J, Jolivet O, Bourroul E, Duroux P (1994) Quantification of hemodynamics in primary pulmonary hypertension with magnetic resonance imaging. Am J Respir Crit Care Med 150(4):1075–1080
20. Prapa M, McCarthy KP, Dimopoulos K, Sheppard MN, Krexi D, Swan L, Wort SJ, Gatzoulis MA, Ho SY (2013) Histopathology of the great vessels in patients with pulmonary arterial hypertension in association with congenital heart disease: large pulmonary arteries matter too. Int J Cardiol
21. Chiu JJ, Usami S, Chien S (2009) Vascular endothelial responses to altered shear stress: pathologic implications for atherosclerosis. Ann Med 41(1):19–28
22. Cunningham KS, Gotlieb AI (2005) The role of shear stress in the pathogenesis of atherosclerosis. Lab Invest 85(1):9–23
23. Efstathopoulos EP, Patatoukas G, Pantos I, Benekos O, Katritsis D, Kelekis NL (2008) Wall shear stress calculation in ascending aorta using phase contrast magnetic resonance imaging. Investigating effective ways to calculate it in clinical practice. Phys Med 24(4):175–181
24. Butler PJ, Weinbaum S, Chien S, Lemons DE (2000) Endothelium-dependent, shear-induced vasodilation is rate-sensitive. Microcirculation 7(1):53–65
25. Shaaban AM, Duerinckx AJ (2000) Wall shear stress and early atherosclerosis: a review. AJR Am J Roentgenol 174(6):1657–1665
26. Bollache E, van Ooij P, Powell A, Carr J, Markl M, Barker AJ (2016) Comparison of 4D flow and 2D velocity-encoded phase contrast MRI sequences for the evaluation of aortic hemodynamics. Int J Cardiovasc Imaging 32(10):1529–1541
27. Bachler P, Valverde I, Pinochet N, Nordmeyer S, Kuehne T, Crelier G, Tejos C, Irarrazaval P, Beerbaum P, Uribe S (2013) Caval blood flow distribution in patients with Fontan circulation:

quantification by using particle traces from 4D flow MR imaging. Radiology 267(1):67–75
28. Moral S, Fernandez-Friera L, Stevens G, Guzman G, Garcia-Alvarez A, Nair A, Evangelista A, Fuster V, Garcia MJ, Sanz J (2012) New index alpha improves detection of pulmonary hypertension in comparison with other cardiac magnetic resonance indices. Int J Cardiol 161(1):25–30
29. Swift AJ, Rajaram S, Hurdman J, Hill C, Davies C, Sproson TW, Morton AC, Capener D, Elliot C, Condliffe R, Wild JM, Kiely DG (2013) Noninvasive estimation of PA pressure, flow, and resistance with CMR imaging: derivation and prospective validation study from the ASPIRE registry. JACC Cardiovasc Imaging